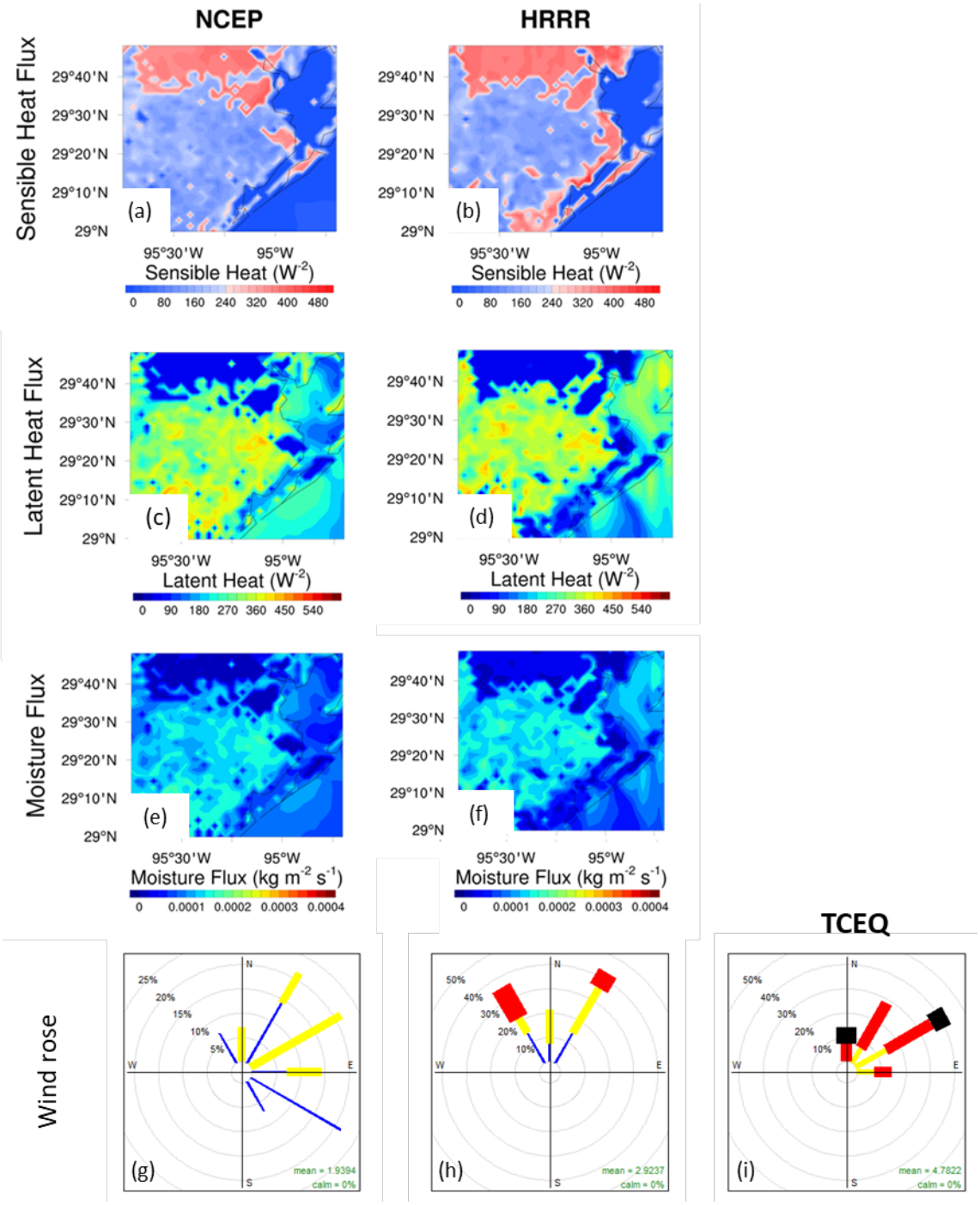

Fig S1: Surface sensible and latent heat fluxes and moisture flux from NCEP FNL and HRRR at 15:00 CDT from the mesoscale domain D02, which are used as initial boundary conditions for the Houston simulations (a-f). The bottom panel shows wind rose plots from NCEP FNL (g), HRRR (h), and TCEQ observations across 14 stations (i).

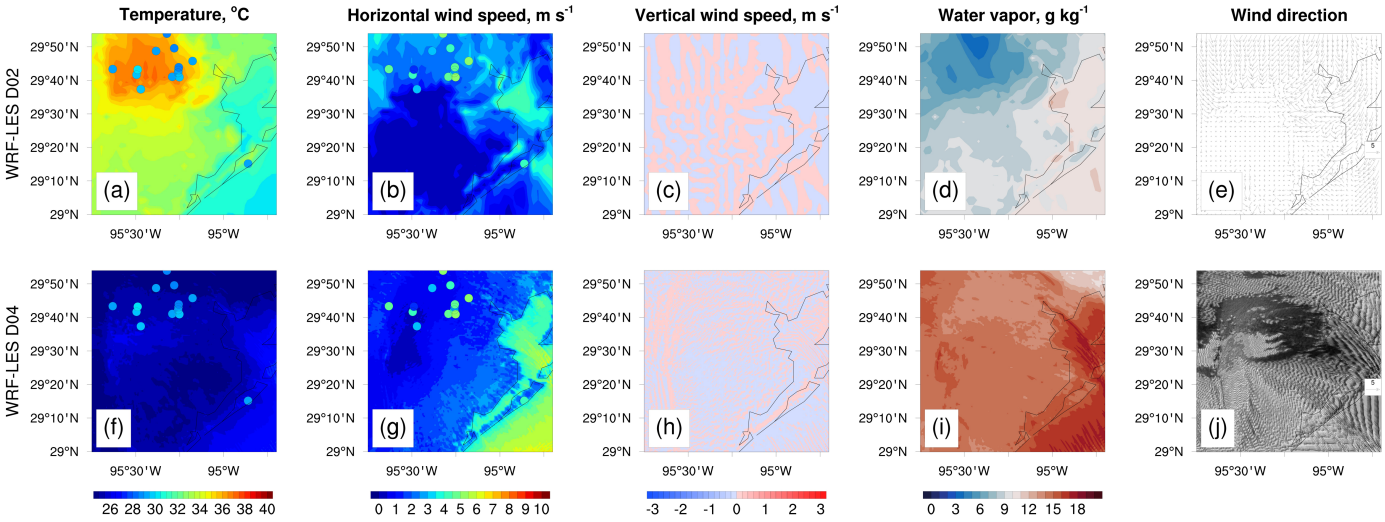

Figure S2: Contour maps are horizontal distributions of simulated temperature (first column), horizontal wind speed (second column), vertical wind speed (third column), water vapor (fourth column), and wind direction (fifth column) near the surface at 09:00 CDT for D02 (first row) and D04 (second row) simulations. Circled dots represent measurements from TCEQ stations.

Table S1: RMSE and MAE for simulated temperature, wind speed, O_3 and NO_2 from domains D02 and D04 in comparison with TCEQ observations.

	Temperature (°C)		Wind speed (m s^{-1})		O_3 (ppbv)		NO_2 (ppbv)	
Deer Park station	**D02**	**D04**	**D02**	**D04**	**D02**	**D04**	**D02**	**D04**
RMSE	2.57	2.39	2.34	2.37	16.01	5.49	3.64	2.29
MAE	1.88	2.08	2.22	2.18	15.05	4.32	3.39	2.01
Clinton station								
RMSE	3.53	2.74	3.03	2.74	11.39	9.52	12.27	2.32
MAE	3.27	2.52	2.91	2.42	9.16	9.21	7.54	2.18

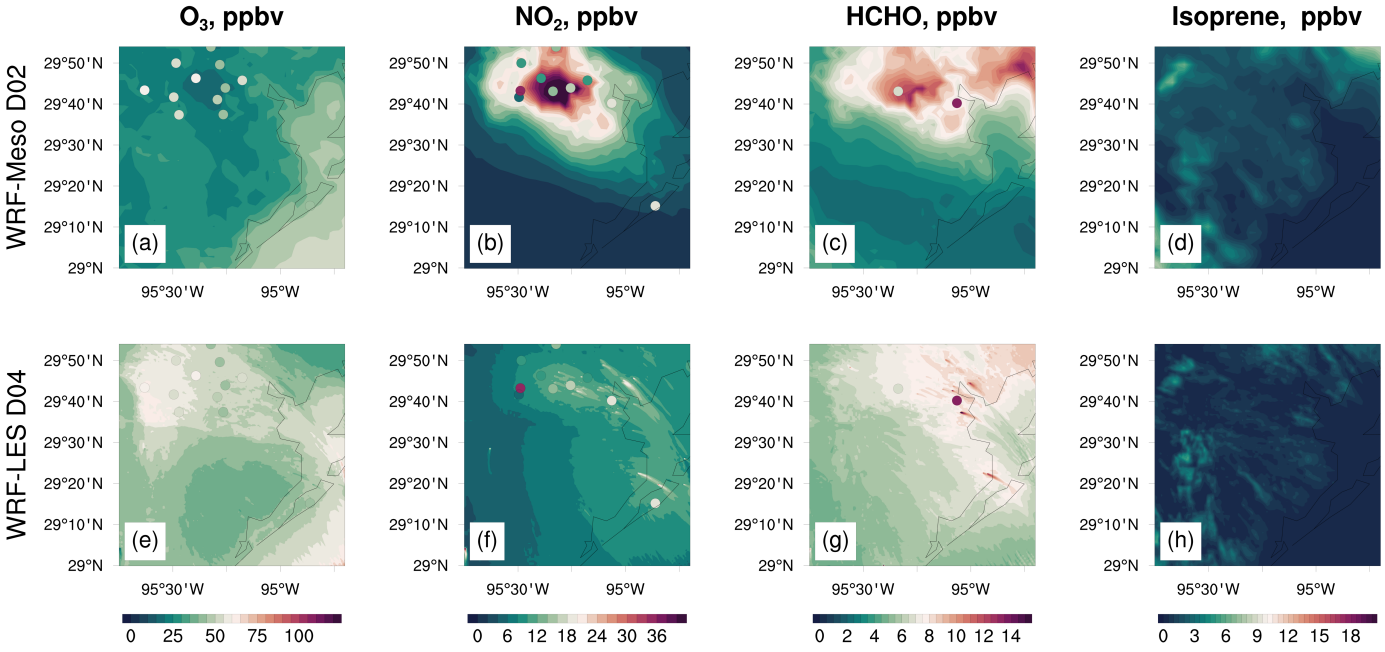

Figure S3: Contour maps are horizontal distributions of simulated O_3 (first column), NO_2 (second column), HCHO (third column) and isoprene (fourth column) near the surface at 09:00 CDT for D02 (first row) and D04 (second row) simulations. Dots represent TCEQ observations of O_3 and NO_2 and Pandora observations of NO_2 and HCHO. Isoprene and other key VOCs are validated separately.

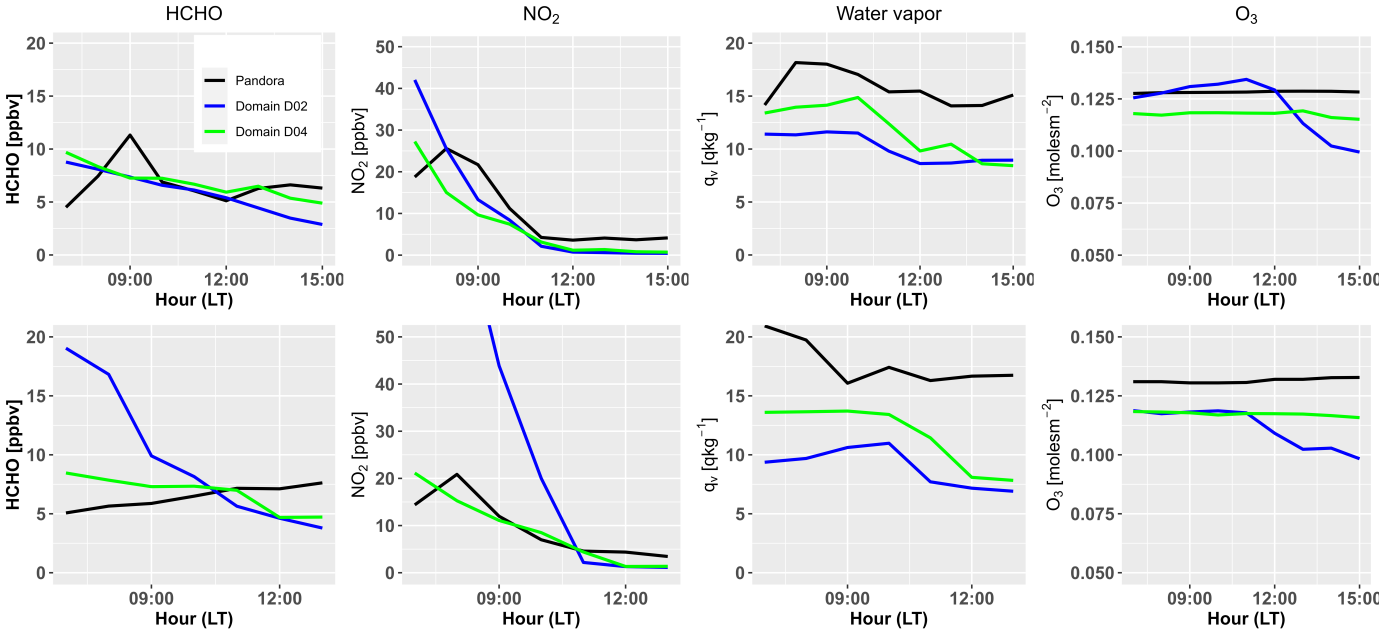

Figure S4: Comparison of simulation results from D02 and D04 with Pandora spectrometer measurements for surface HCHO, surface NO_2, surface water vapor (q_v) and total column O_3. The upper panel represents comparison for the La Porte Pandora station; the lower panel is for the University of Houston station.

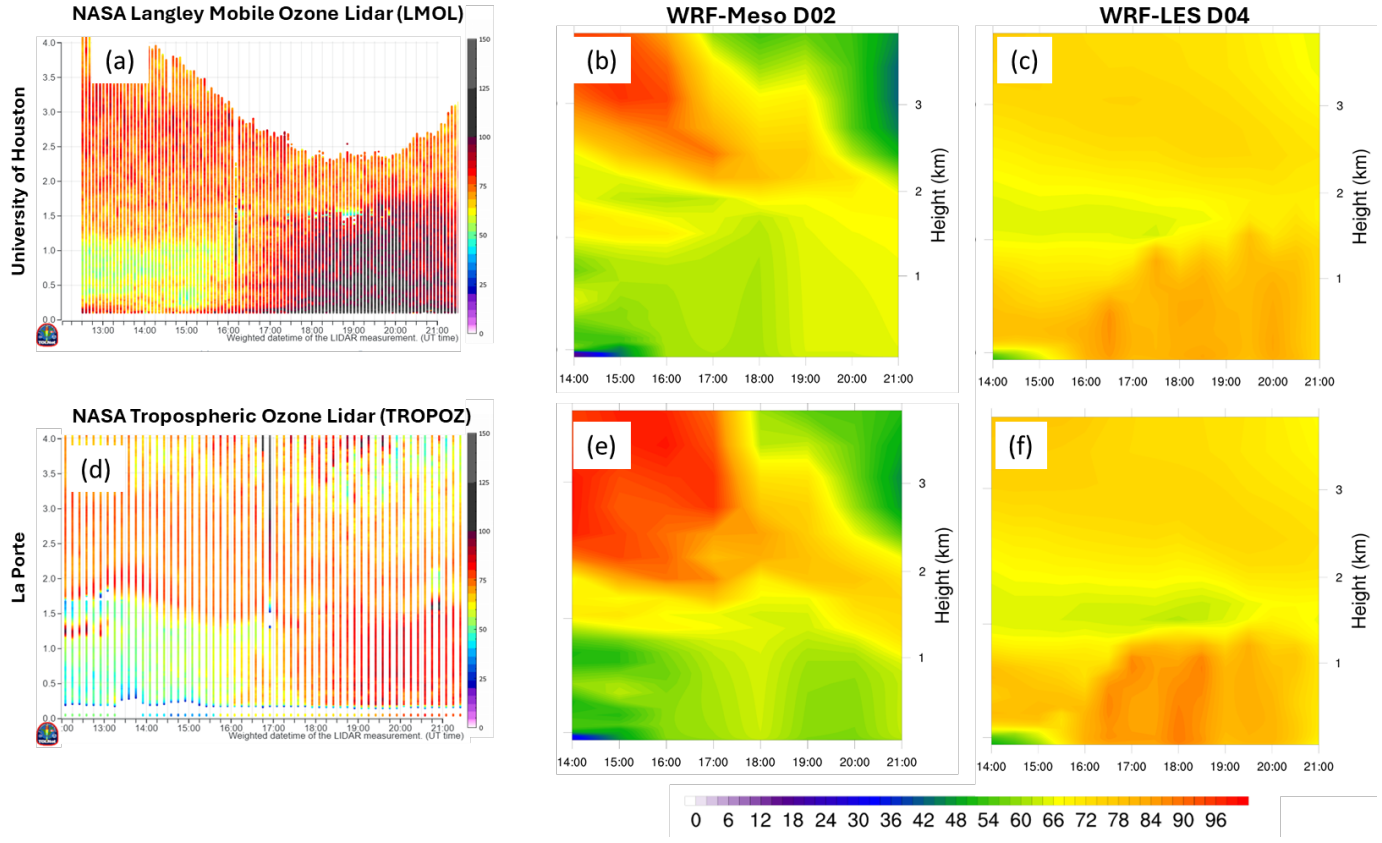

Figure S5: Vertical cross sections of the temporal evolution of ozone profiles (ppbv) from (a) the ground-based Lidar measurements from the NASA TRACER-AQ campaign (figure plotted from https://tolnet.larc.nasa.gov/), (b) model results from the mesoscale domain D02, and (c) model results from the LES domain D04. The upper left panel represents data from the University of Houston LMOL site (29.724° N, 95.3392° N) available from 12:30 UTC (September 8, 2021) to 00:00 UTC (September 9, 2021), and the lower left panel represents the La Porte TROPOZ site (29.667° N, 95.064° N) available from 00:00 UTC (September 8, 2021) to 00:00 UTC (September 9, 2021). All time units are in UTC to match with NASA LMOL measurements.

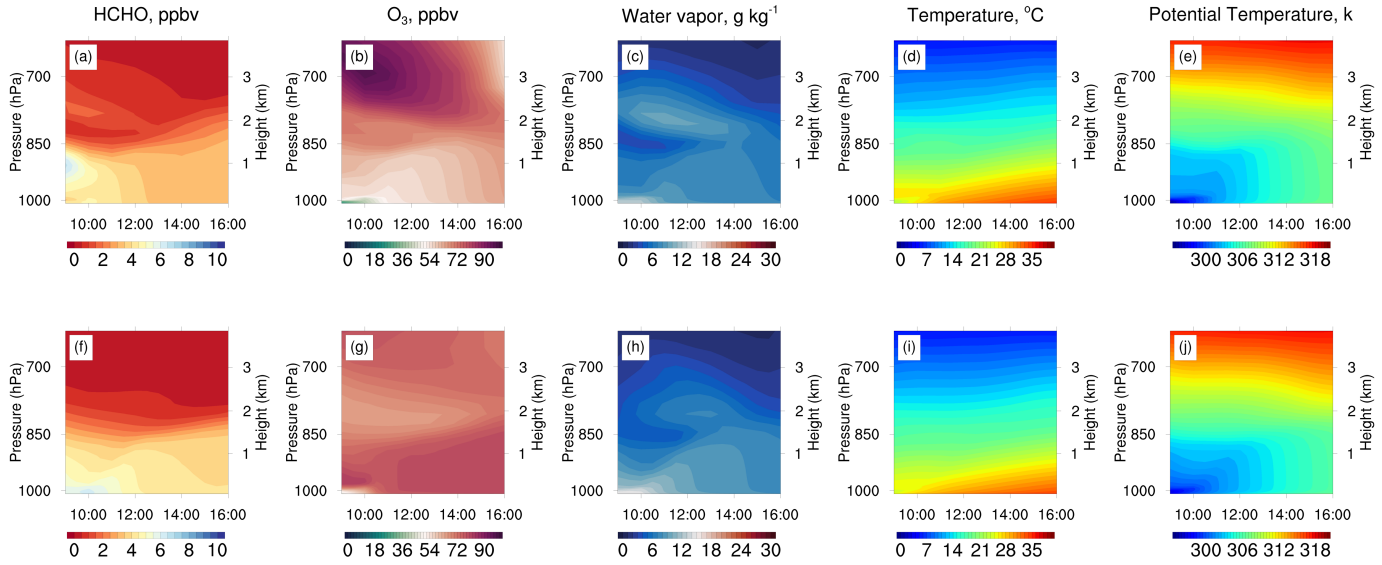

Figure S6: Vertical cross-sections of the temporal evolution (time in CDT) of (a) HCHO, (b) O_3, (c) water vapor, (d) temperature and (e) potential temperature profiles over the LES domain D04 with a focus on the land area. The upper panel represents simulation from the Mesoscale domain D02; the lower panel is for the LES domain D04.

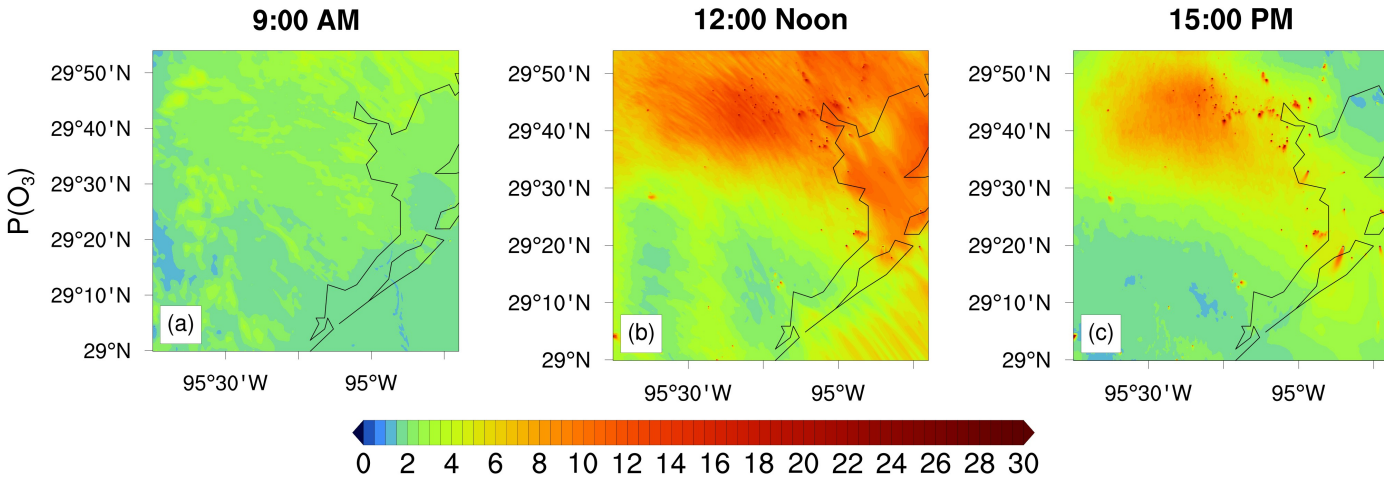

Figure S7: Spatial distribution of ozone production rate (PO_3) in ppbv h^{-1} at (a) 09:00 CDT, (b) 12:00 CDT and (c) 15:00 CDT.

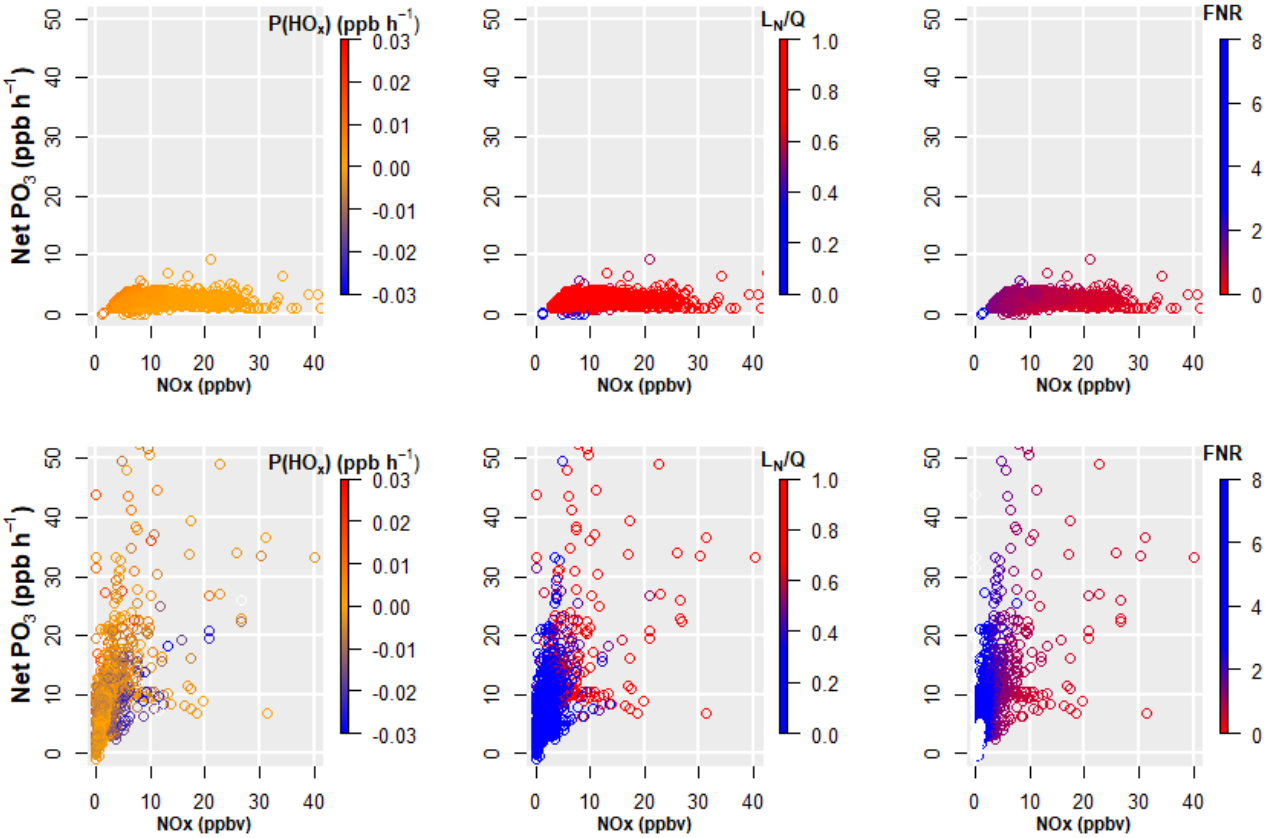

Figure S8: Production rate of HO_X ($OH+HO_2$) (first column), L_N/Q (second column) and FNR (third column) as a function of net O_3 production rate and NO_X ($NO + NO_2$) mixing ratio at 09:00 CDT (first row) and 15:00 CDT (second row). Individual data points represent all grid cells from the LES domain at the surface.

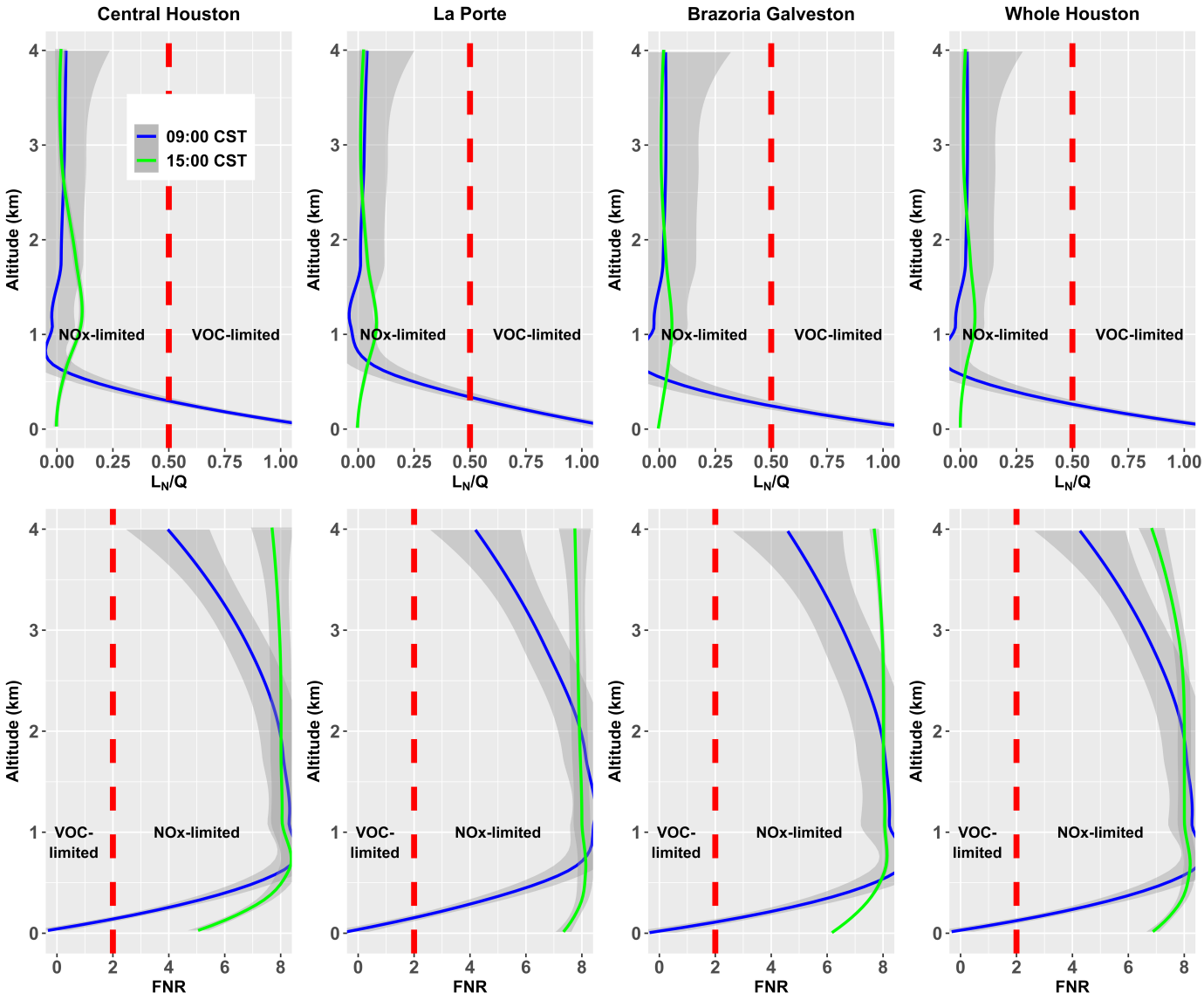

Figure S9: Vertical profiles of L_N/Q (first row) and FNR (second row) at 09:00 CDT (blue) and 15:00 CDT (green) over Central Houston (first column), La Porte (second column), Brazoria-Galveston (third column) and Whole Houston (fourth column) regions.

Table S2: Loss rate of selected chemical species through photolysis (pptv s^{-1})

Compounds	Photolysis reactions	12:00 CDT	15:00 CDT
Hydrogen peroxide	H_2O_2 + hv	0.039331	0.05058
Ozone	O_3 + hv	32.29377	36.29043
Nitric acid	HNO_3 + hv	0.001839	0.001445
Pernitric acid	HO_2NO_2 + hv	5.04E-05	0.000022
Nitrate	NO_3 + hv	0.047363	0.02942
Bicyclic hydroperoxide	BENZOOH + hv	3.12E-07	0.000001
Lumped aldehydes	BIGALD + hv	0.000759	0.001538
Ethyl hydroperoxide	C_2H_5OOH + hv	2E-05	0.00004
Propyl hydroperoxide	C_3H_7OOH + hv	2.01E-05	0.000037
Phenyl hydroperoxide	C_6H_5OOH + hv	6.4E-06	0.000018
Formaldehyde	HCHO + hv	0.14231	0.127699
Acetaldehyde	CH_3CHO + hv	0.004351	0.003849
Acetone	CH_3COCH_3 + hv	0.004491	0.005341
Methyl glyoxal	CH_3COCHO + hv	0.032041	0.028678
Peracetic acid	CH_3COOOH + hv	0.000345	0.000791
Acetic acid	CH_3OOH + hv	0.003911	0.006042
Glycolaldehyde	C_2H_4O + hv	0.003949	0.006003
Glyoxal	$C_2H_2O_2$ + hv	0.016825	0.016722
Methacrolein	C_4H_6O + hv	0.001142	0.001737
Methyl ethyl ketone	$CH_3CH_3COCH_2CH_3$ + hv	0.00072	0.000627
Methyl vinyl ketone	$CH_3C(O)CH=CH_2$ + hv	0.000705	0.001095
Acetone hydroperoxide	ROOH + hv	5.51E-05	0.000125
Peroxy acetyl nitrate	PAN + hv	0.000418	0.000276

Table S3: Total Reactivity (s^{-1}) of selected compounds with OH, O_3 and NO_3 averaged over different focus regions.

Oxidants	Compounds	Central Houston	La Porte	Brazoria	Whole Houston
OH	Alkanes	0.39 ± 0.19	0.36 ± 0.21	0.36 ± 0.15	0.3 ± 0.12
	Alkenes	0.45 ± 0.22	0.47 ± 0.30	0.25 ± 0.16	0.28 ± 0.16
	Aromatics	0.1 ± 0.07	0.09 ± 0.07	0.03 ± 0.02	0.05 ± 0.03
	OVOCs	1.61 ± 0.77	1.73 ± 0.91	1.57 ± 0.7	1.36 ± 0.59
	CH_4	0.22 ± 0.11	0.2 ± 0.11	0.27 ± 0.13	0.2 ± 0.09
	CO	0.93 ± 0.47	0.82 ± 0.49	0.9 ± 0.39	0.72 ± 0.29
	NMVOC	5.73 ± 2.51	4.73 ± 2.11	2.21 ± 0.97	3.45 ± 1.39
	NO_X	0.48 ± 0.35	0.5 ± 0.45	0.37 ± 0.33	0.34 ± 0.27
	O_3	0.09 ± 0.05	0.08 ± 0.05	0.12 ± 0.06	0.08 ± 0.04
	SO_2	0.04 ± 0.02	0.06 ± 0.04	0.05 ± 0.03	0.04 ± 0.02
NO_3	NMVOC	0.039 ± 0.011	0.029 ± 0.007	0.003 ± 0.002	0.02 ± 0.005
	NO_X	0.22 ± 0.37	0.25 ± 0.43	0.336 ± 0.95	0.23 ± 0.56
	Alkenes	0.002 ± 0.002	0.001 ± 0.003	0.001 ± 0.001	0.0009 ± 0.001
	OVOCs	0.0002 ± 0.0006	0.0003 ± 0.0007	0.0003 ± 0.0009	0.0002 ± 0.0006
O_3	NMVOC	0.44 ± 0.25	0.33 ± 0.17	0.06 ± 0.008	0.35 ± 0.19
	NO_X	0.71 ± 0.47	0.72 ± 0.54	0.48 ± 0.44	0.49 ± 0.38
	Alkenes	0.046 ± 0.016	0.054 ± 0.02	0.026 ± 0.017	0.03 ± 0.01
	OVOCs	0.015 ± 0.008	0.016 + 0.009	0.008 ± 0.004	0.01 ± 0.006

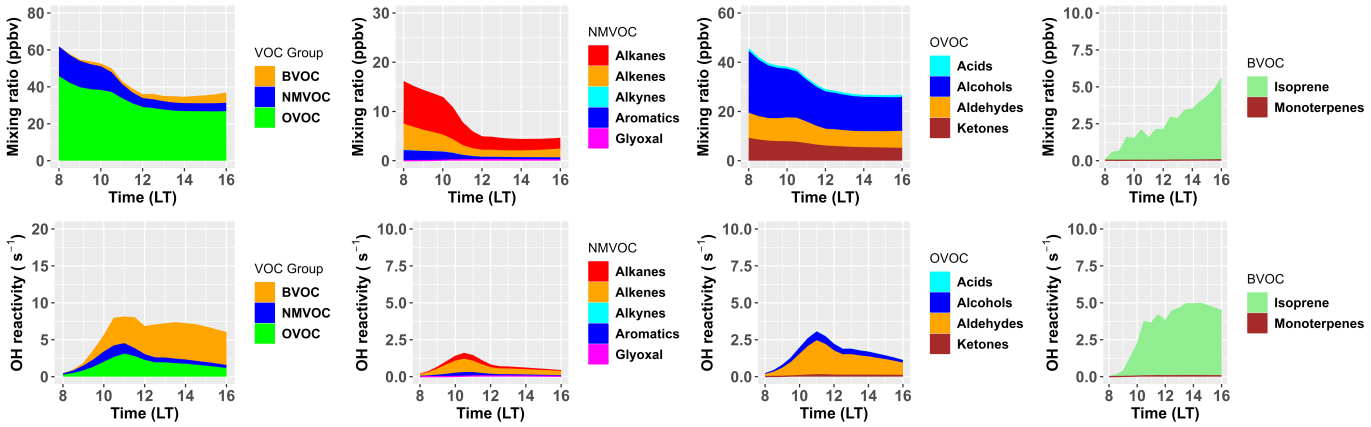

Figure S10: Diurnal variations of VOC mixing ratio and OH reactivity averaged over Central Houston from the LES D04 domain for (a) all VOC group, (b) NMVOC, (c) OVOC and (d) BVOC.

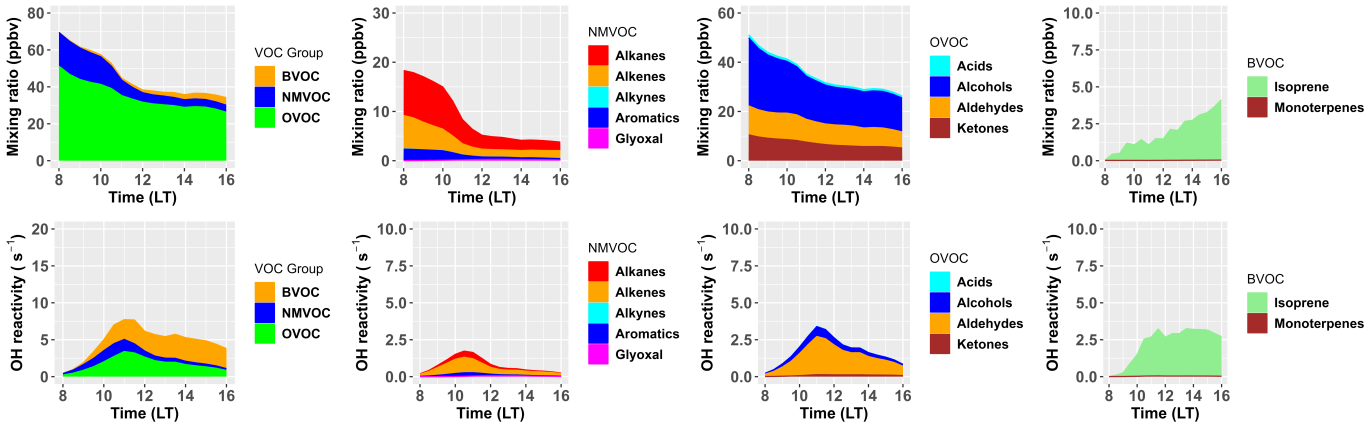

Figure S11: Diurnal variations of VOC mixing ratio and OH reactivity averaged over La Porte from the LES D04 domain for (a) all VOC group, (b) NMVOC, (c) OVOC and (d) BVOC.

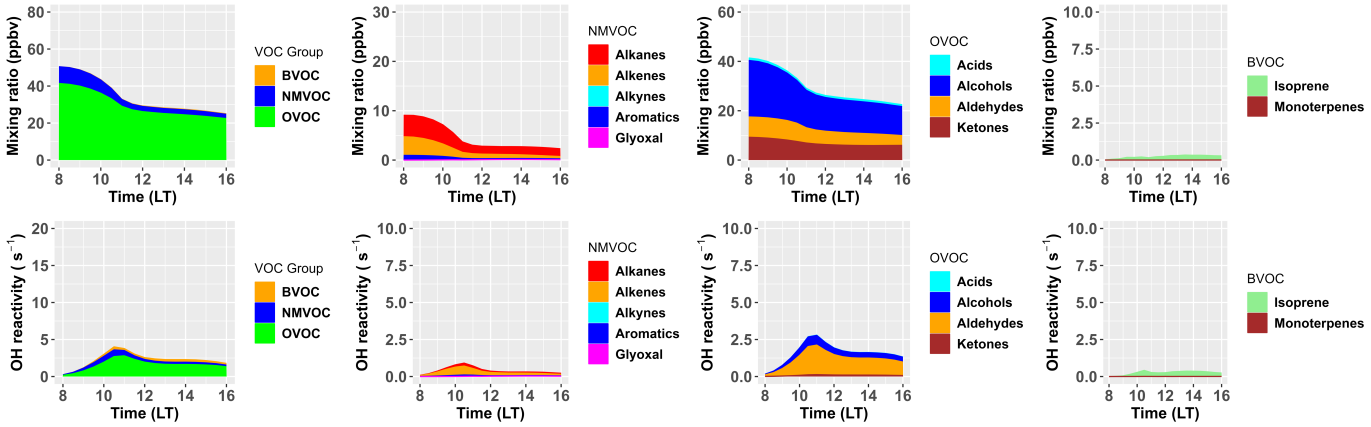

Figure S12: Diurnal variations of VOC mixing ratio and OH reactivity averaged over Brazoria-Galveston from the LES D04 domain for (a) all VOC group, (b) NMVOC, (c) OVOC and (d) BVOC.